

## CT Review of ovarian fibrothecoma

Pat, J. Rothnie, K. Kolomainen, D. Sundaresan, M. Zhang, J. Liyanage, S.

## Introduction:

Ovarian fibrothecoma are rare types of stromal tumours classified under the thecoma-fibroma group, which accounts for 4% of all ovarian cancers<sup>(1,2)</sup>. These typically present in post-menopausal women in their 5<sup>th</sup> to 6<sup>th</sup> decade<sup>(3)</sup>. These tumours are subdivided into fibromas, fibrothecomas and thecomas, each corresponding to the presence of their histological makeup<sup>(4)</sup>. In situations where these tumours share overlapping histological characteristics, they're denoted as fibrothecomas<sup>(5,6)</sup>. Despite rise of CT use in recent decades, ovarian malignancies are often misdiagnosed due to their varying CT appearances on cross-sectional imaging and association with increased serum carbohydrate antigen-125 (CA-125) levels<sup>(7-13)</sup>.

Serous papillary carcinomas (SPC) are classified under the epithelial ovarian cancers (EOC) group. This accounts for 75% of ovarian cancers and is associated with typical CT features of ascites, peritoneal involvement and varying sizes of ovarian mass<sup>(14-19)</sup>. Another common EOC includes ovarian endometrioids (EM) which accounts for 8-15% of all ovarian cancers and is characterised by solid-cystic masses on cross-sectional imaging<sup>(20-24)</sup>.

Over recent decades, the multidisciplinary management approach (MDM) has played a crucial role within UK's National Institute of Clinical Excellence (NICE) to provide optimal care for patients<sup>(25,26)</sup>. Occasionally fibrothecomas can often be mistaken as ovarian malignancies and referred to oncological tertiary centre MDMs<sup>(27)</sup>. Mistaking benign ovarian tumours as malignancy and subsequent MDM referrals can result in time and financial burden on the NHS.

The incidences of ovarian fibrothecomas are rare, thus only limited data are available in the literature. In light of this, the primary aim of our study is to identify the salient CT imaging features of histologically-proven fibrothecoma in order to guide accurate diagnosis. Additionally we also aim to analyse CT characteristics that could aid in differentiating fibrothecoma from early-stage SPC malignancies. To the extent of our knowledge, we currently hold the largest histologically-proven sample size of fibrothecoma lesions for radiological analysis.

## Methodology

This study was carried out retrospectively, analysing fibrothecoma patient groups from January 2013 to December 2021 and EOC patient groups from January 2019 to December 2021. Both the radiologist and histopathologists were blinded in their review of cases.

### Patient population

A retrospective search identified a total of 85 female patients. These patients all had their initial investigation performed within Mid and South Essex (MSE) NHS Foundation Trust. Consent is obtained for each patient prior to every CT study. These were subdivided into 3 separate patient groups: fibrothecoma; SPC; and EM. Samples for fibrothecoma were obtained across the region of three MSE hospital sites. The EOC samples were only taken locally in Southend University Hospital. Doing so allowed us to match the sample size and population of the control and study group. The clinical signs and symptoms were reviewed using the hospital's electronic medical records. All patients underwent radical surgical resection and each ovarian mass was histologically confirmed as either fibrothecoma, SPC or EM. Serum CA-125 was also analysed in the biochemistry department for additional clinical correlation. All clinical information and electronic medical records was reviewed by the radiology registrar (JP).

### CT scan protocol

Two GE scanners were utilised between 2013-2021 (GE VCT lightspeed and GE Rev EVO). Each patient received Omnipaque 300 (Iohexol) contrast at 1.5ml/kg in 35ml saline with a flow rate of 2.5-4ml/s. Image acquisition was obtained with a delay of 70 seconds post contrast injection, acquiring 0.625mm slices at 0.8 seconds tube rotation (Pitch – 1.375:1).

The image raw data was then transferred onto a GE workstation for processing and reconstruction. These were then transferred onto the Insignia Medical Systems Viewer for multiplanar viewing and analysis.

### Image Analysis

All images were analysed by an experienced uro-gynaecological consultant radiologist (SL) with over 10 years of experience and a radiology registrar (JP). Observations were conducted on all 3 groups, each ovarian lesion interrogated with specific attention to the following: ① Laterality; ② shape; ③ margins; ④ size; ⑤ calcification; ⑥ structural configuration; ⑦ CT Hounsfield unit (HU) of the solid component of the mass (if present), myometrium of uterus and psoas; ⑧ presence of endometrial thickening (>4mm) (to assess the effect of oestrogen production) and ⑨ other radiological signs (ascites, pleural effusion, enlarged lymph nodes and peritoneal disease).

The HU density value of the masses' solid component was compared with the density of the uterus and psoas muscle. This is represented as 'density ratio' demonstrated below:

$$\text{Mass: Psoas Density Ratio} = \frac{\text{Mean HU of Lesion}}{\text{Mean HU of Psoas}} \quad (1)$$

$$\text{Mass:uterus Density Ratio} = \frac{\text{Mean HU of Lesion}}{\text{Mean HU of Uterus}} \quad (2)$$

In cases where the tumour only demonstrated a purely cystic appearance, the HU value of the cystic component was sampled instead. For each lesion, three regions of interest (ROI) were placed at different solid components of the mass; the highest HU value of three was selected. Areas of visible blood vessels, fibroids and cystic components were avoided.

### Pathology Examination

All cases between the groups underwent basic H&E staining for morphological analysis. Histological appearances of fibromas and thecomas comprise discrete spindle cells within collagen, as opposed to packets of clear cells. Special stain for collagen (Martius scarlet and blue) was used to accentuate the difference (**Figure 1**). Control cases of epithelial malignancies were also examined radiologically. The MSB stained sections were assessed for proportions of fibroma to thecoma. Histological analysis was analysed by the histopathologists in Mid South Essex NHS Foundation Trust with lead consultant histopathologist (MS). There was no discordance during the analysis of the data.

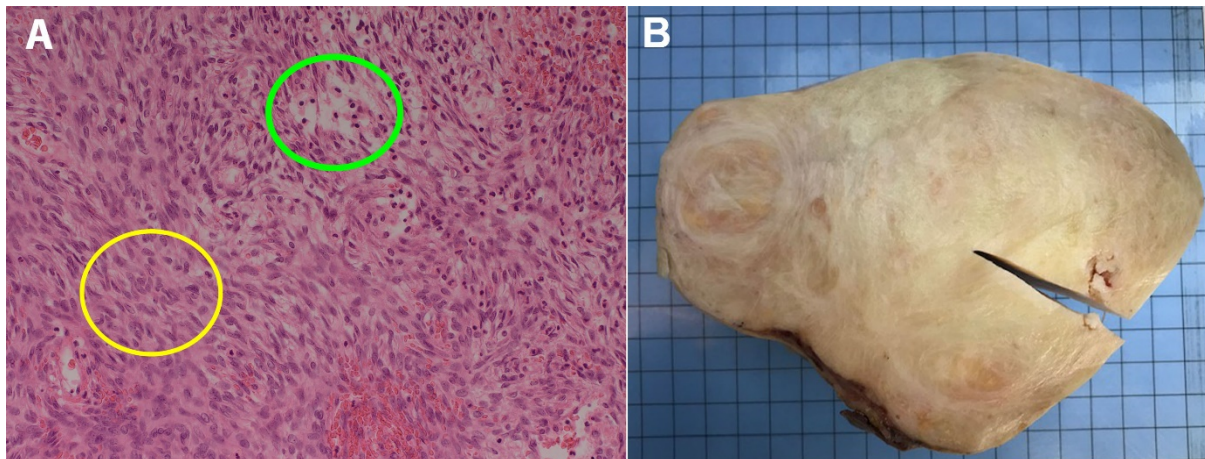


**Figure 1:**

**A:** High power (x200) histological slice.

- (Yellow bottom Circle) Fibromatous area comprising spindle cells with individual cells surrounded by pink collagen.
- (Green upper Circle) Cluster of thecomatous cells with pale cytoplasm and arranged in clusters. Clarity due to theca cell associated fat oestrogen-based products

**B:** Macro section of the ovarian fibrothecoma mass.

### Statistics

Continuous data are presented as mean and the standard deviation or median and the inter-quartile ranges and categorical variables are expressed as percentages. The independent t-test or the Mann-Whitney U test was used to compare the difference between two continuous variables depending on the distribution of data. The Chi-square test or Fisher's exact test was used to assess the association between two categorical variables. Penalized logistic regression models were performed to provide an easy way to interpret the results (Mass:PsoasRatio and Mass:UterusRatio). The

CT Review of Ovarian fibrothecoma

Hosmer-Lemeshow goodness of fit tests was used to evaluate the model fit. A 5% significance level was used (two-tailed). The STATA statistical computer package was used to analyse the data.

## Results

### Clinical data

A total of 85 patients (108 lesions) were analysed, each categorised under the cohorts of fibrothecoma, SPC and EM, comprising of 36 (41 lesions), 36 (52 lesions) and 13 (15 lesions) patients respectively. Average age among all three arms was 66.2 ( $\pm 11.4$ ). All patients were menopausal except for 7 women who were of perimenopausal or premenopausal status. 22 patients did not have pre-procedural CA-125 investigation. Of the patients that had CA-125 results, 52 returned with abnormal results (Normal:  $\leq 35$  U/ml) (**Table 1**).

### CT findings

#### Fibrothecoma data

The average age was 67.8 years; all reached menopausal status except for one who was undergoing perimenopause. There were 36 patients with 41 fibrothecoma lesions. 22 were unilateral, 5 were bilateral and 9 were indeterminate. Shape analysis showed 26 was lobulated, 7 were round and 8 were oval. The largest diameter measured was 24.7cm with a median value of 10cm (IQR: 6.9-12.7cm). Only 3 cases showed calcifications within this cohort. 29 patients had ascites of varying degrees, 5 patients had pleural effusion and 4 had peritoneal fat stranding. None of the patients showed positive signs of lymphadenopathy. 5 patients had a hysterectomy and therefore uterine analysis could not be performed.

The densities of 41 lesions were measured with a HU average of  $43.95 \pm 11.17$  (**Figure 2**). These were compared separately with the density of the psoas muscle and uterus as internal references (Equation 1 and 2). The mass to density ratio between the psoas muscle and uterus showed a median of 0.7 (IQR 0.6-0.9) and 0.5 (IQR 0.5-0.7) respectively (**Table 2** and **Figure 3**). Both 'Mass:Psoas ratio' and 'Mass:Uterus ratio' values were less than 1 which was a statistically significant finding ( $p < 0.0001$  and  $p < 0.001$  respectively).

We analysed the structural configuration for each lesion according to its solid or cystic characteristics (**Table 2**). 18 of 41 lesions were found to be purely solid and only two lesions demonstrated purely cystic characteristics in the fibrothecoma cohort (**Figure 4**). Additionally, the size of the tumour was also analysed against the degree of ascites and the structural configuration of the mass (**Figure 5**).

## CT Review of Ovarian fibrothecoma

<b>Table 1 – Clinical data</b>					
Patient Data	Fibrothecoma (n=36)	Serous Papillary Carcinoma (n=36)	p-value	Serous Papillary Carcinoma mimics (n=12)	p-value (mimics)
Age (mean (SD)), range, yrs	67.8 (11.46), [48-89]	66 (10.9), [36-86]	0.6	66.1 (10.3), [46-83]	0.6
Menopause			0.2		0.4
Non-menopausal	0	2 (11.1%)		1 (8.3%)	
Menopause	35 (97.2%)	18 (86.1%)		8 (91.7%)	
Perimenopause	1 (2.8%)	1 (2.8%)		0	
Ca-125 – n (%),			0.16		0.35
<=35	7 (19.4%)	3 (8.3%)		0 (0%)	
>35	21 (58.3%)	29 (80.6%)		9 (75.0%)	
Not done/unavailable	8 (22.2%)	4 (11.1%)		3 (25.0%)	
Ascites – n (%)			0.29		0.01
No Ascites	7 (19.4%)	10 (27.8%)		8 (66.7%)	
1+	11 (30.6%)	6 (16.6%)		3 (25%)	
2+	11 (30.6%)	8 (22.2%)		0 (0%)	
3+	7 (19.4%)	12 (33.3%)		1 (8.3%)	
Pleural effusion – n (%)			0.53		0.31
Positive	5 (13.9%)	7 (19.4%)		0 (0%)	
Negative	31 (86.1%)	29 (80.6%)		12 (100%)	
Lymphadenopathy – n (%)			<0.001		--
Positive	0 (0%)	12 (33.4%)		0 (0%)	
Negative	36 (100%)	24 (66.6%)		9 (100%)	
Peritoneal disease – n (%)			<0.001		0.09
Positive	4 (11.1%)	26 (72.2%)		4 (33.3%)	
Negative	32 (88.9%)	10 (27.8%)		8 (66.7%)	
Location – n (%)			0.047		0.05
Right	15 (41.7%)	8 (22.2%)		3 (25.0%)	
Left	7 (19.4%)	4 (11.1%)		0 (0%)	
Bilateral	5 (13.9%)	15 (41.7%)		6 (50.0%)	
Indeterminate	9 (25.0%)	9 (25.0%)		3 (25.0%)	
Patients with a uterus	Fibrothecoma (n=31)	Serous Papillary Carcinoma(n=31)	p-Value		
Thickened endometrium			0.26		0.65
Thickened (>=4mm)	12 (38.7%)	6 (19.4%)		2 (18.2%)	
Not thickened (<4mm)	19 (61.3%)	23 (74.1%)		9 (81.8%)	

**Table 1:** Patient clinical data of both FBT and SPCs with p-values. Bottom of the table demonstrates patients with a thickened endometrium who have not undergone a hysterectomy procedure. *n* = number of patients

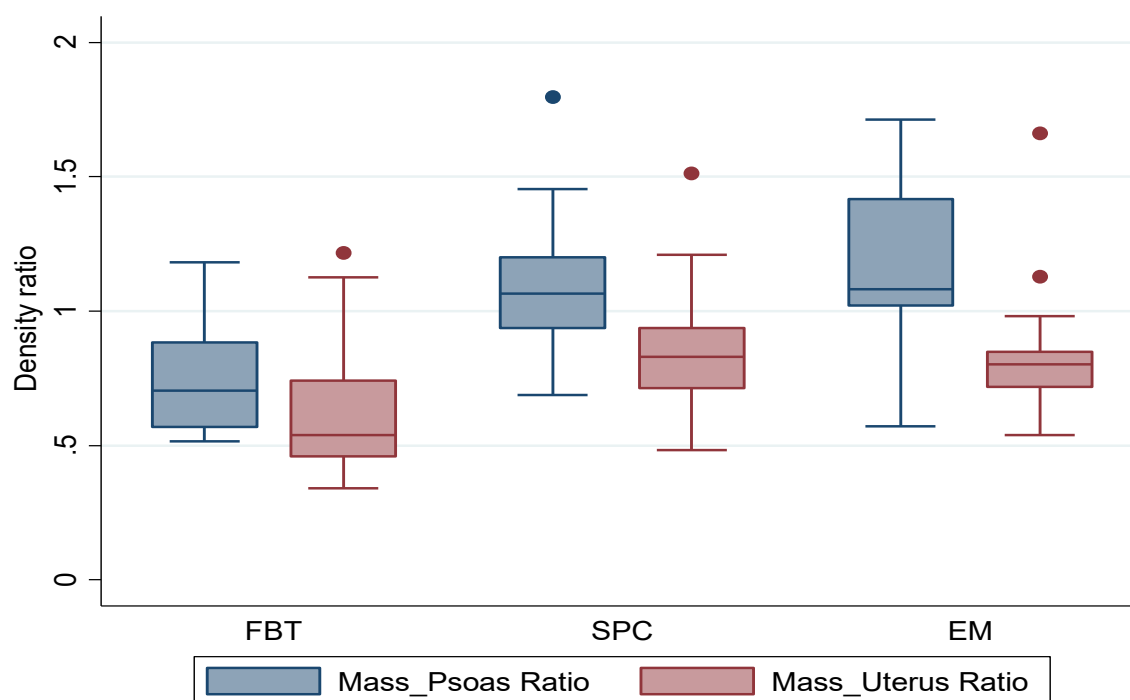


**Figure 2:** Boxplot illustrating the range of HU density between the psoas muscle, uterus and the solid component of each corresponding ovarian mass.

FBT - Fibrothecoma, SPC – Serous Papillary Carcinoma, EM – Endometrioid carcinoma

#### Serous Papillary Carcinoma Data

The second cohort had 36 histologically confirmed serous papillary carcinoma lesions. The average age was 66 years and all patients had reached menopause except for 5 who was premenopausal and 1 perimenopausal. Each excised tumour were staged under the FIGO (International Federation of Gynaecology and Obstetrics) staging criteria in subsequent histology described in **table 3**. There were 3 patients at stage 1, 5 patients at stage 2, 25 patients at stage 3 and 3 patients at stage 4. Lesion analysis showed 12 were unilateral, 15 bilateral and 9 were indeterminate. The size across 3 planes showed a median of 7.5cm (IQR: 4.8-11.2) (largest lesion: 24cm). 26 patients had a degree of ascites, 7 patients demonstrated signs of pleural effusion, 12 patients had lymphadenopathy and 26 patients had evidence of peritoneal disease. A total of 31 patients had a uterus and only 6 had a thickened endometrium.

All lesions had well defined margins except for 9 which were ill-defined. The tumour structural configuration is illustrated in **figure 6**. 7 SPC lesions showed calcification. The average HU of the lesions and the *mass to psoas HU ratio* were  $66.8 \pm 14.96$  and  $1.12 \pm 0.23$  ( $p < 0.0001$ ) respectively. The *mass to uterus ratio* was  $0.9 \pm 0.21$  ( $p < 0.001$ ).

FIGO staging class	Number of SPC patients
1	3
2	5
3	25
4	3

Table 3: Breakdown of SPC patients with their corresponding FIGO staging on final histology



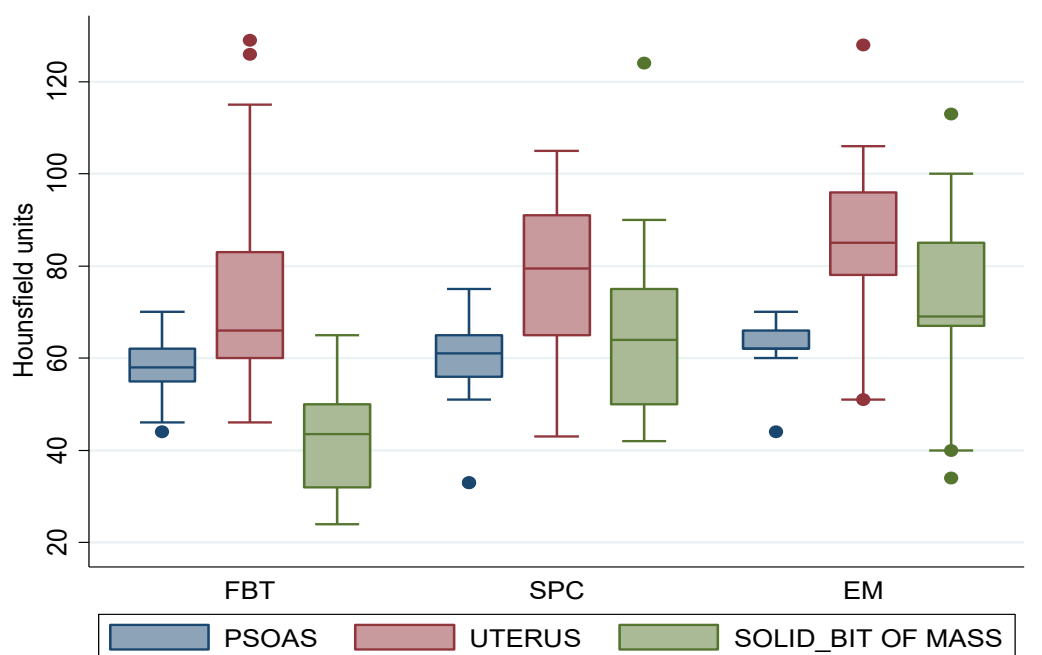


**Figure 3:** Boxplot of Mass to Psoas (blue) and Mass to Uterus (Red) density ratios of the three ovarian masses.

FBT - Fibrothecoma, SPC – Serous Papillary Carcinoma, EM – Endometrioid carcinoma

A specific subset of SPCs were analysed separately as they showed features closely related to fibrothecomas. These tumours were deemed to be '*mimics*', demonstrating FIGO staging 1 to early 3 without disseminated disease. A total of 12 patients (18 lesions) were identified to be mimics with comparisons seen on **table 1 and 2**. Despite the reduced sample size, our data continue to show similar statistically significant findings for cystic configuration tendency ( $p=0.001$ ) with a *mass to psoas* or *mass to uterus ratio* of greater than 1 ( $p<0.0001$ ).

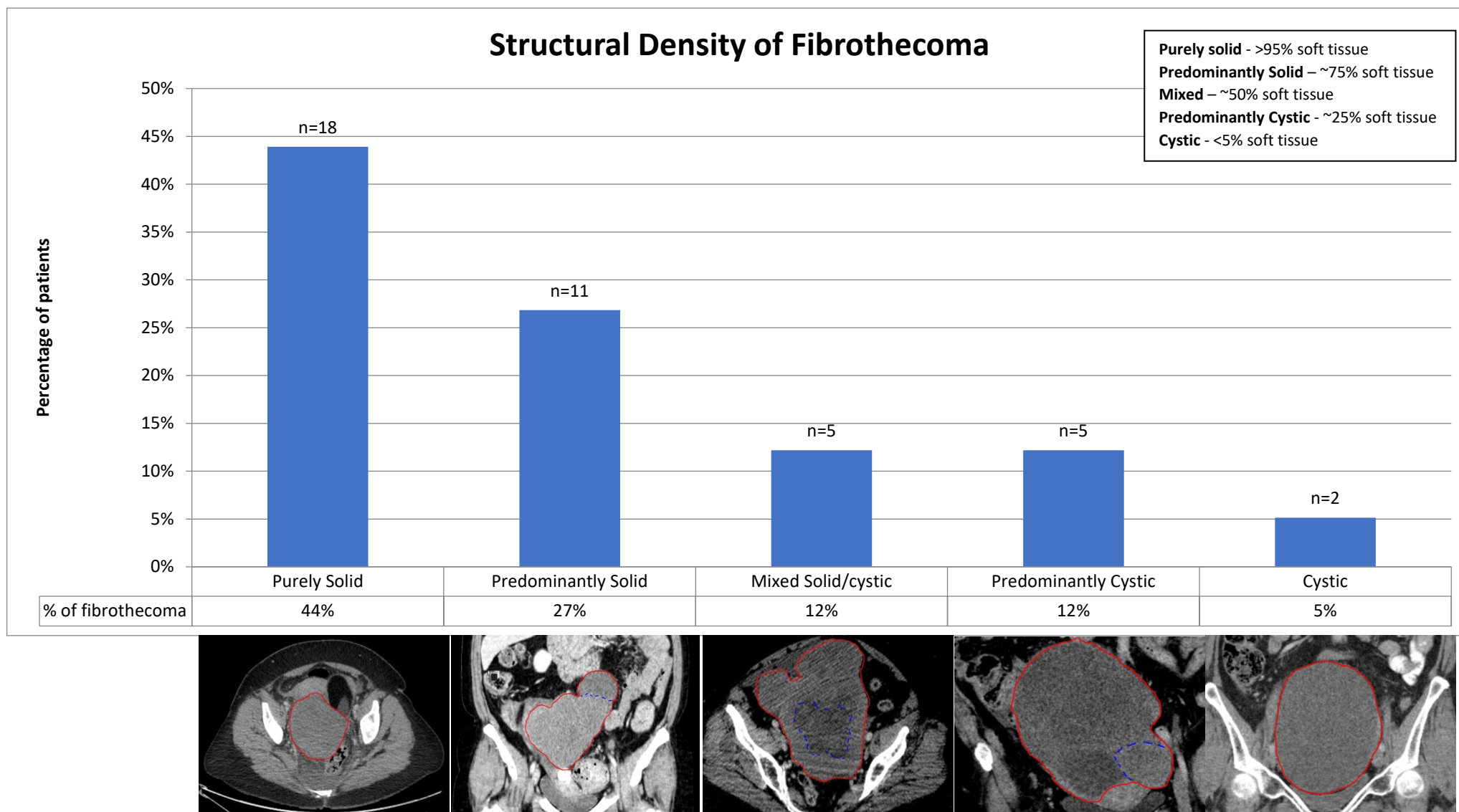
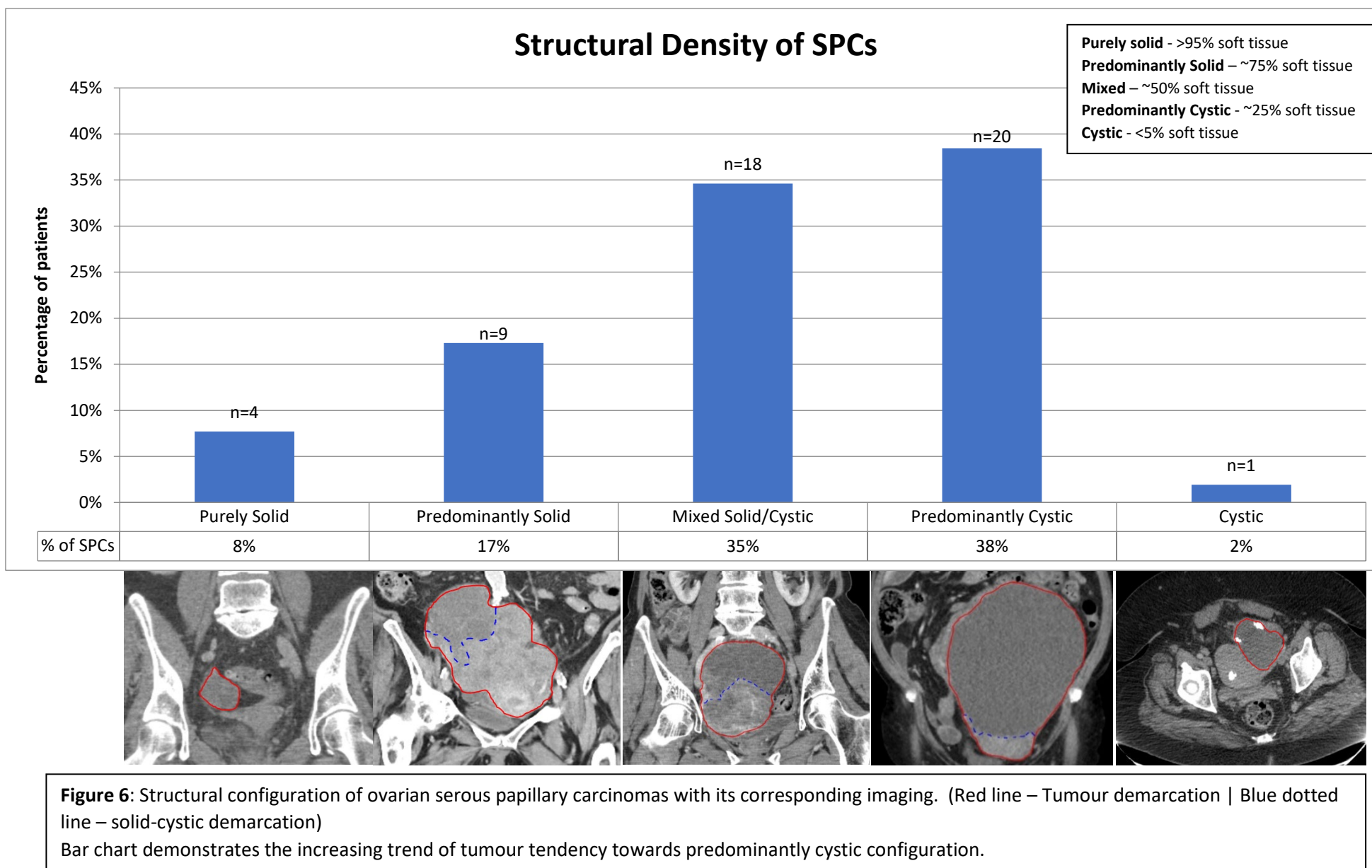


**Figure 4:** Structural configuration of fibrothecoma with its corresponding imaging. (Red line – Tumour demarcation | Dotted Blue line – Solid-cystic demarcation) Demonstrating the tumour’s tendency to favour solid configuration.



<b>Table 2 - CT Findings</b>					
	<b>Fibrothecoma (n=41)</b>	<b>SPC (n=52)</b>	<b>p-value</b>	<b>SPC mimics (n=18)</b>	<b>p-value</b>
<b>Size - median (IQR)</b>	9.4 (6.9-12.7)	7.5(4.8-11.1)	0.12	9.0 (6.4-12.7)	0.83
<b>Shape- n(%)</b>			<b>0.001</b>		0.05
Lobulated	26 (63.4%)	47 (90.4%)		17(94.4%)	
Oval	8 (19.5%)	5 (9.6%)		1 (5.6%)	
Round	7 (17.1%)	0 (0%)		0 (0%)	
<b>Margins – n(%)</b>			<b>0.01</b>		0.31
Well-defined	41 (100%)	43(82.7%)		16 (88.9%)	
Ill-defined	0 (0%)	9 (17.3%)		2 (11.1%)	
<b>Calcification – n(%)</b>			0.5		0.18
	3 (7.3%)	7 (13.5%)		4 (22.2%)	
	38 (92.7%)	45 (86.5%)		14 (77.8%)	
<b>Density – n(%)</b>			<b>&lt;0.001</b>		<b>&lt;0.001</b>
Purely Solid	18 (43.9%)	4 (7.7%)		1 (5.6%)	
Predominantly Solid	11 (26.8%)	9 (17.3%)		1 (5.6%)	
Mixed	5 (12.2%)	18 (34.6%)		6 (33.2%)	
Predominantly Cystic	5 (12.2%)	20 (38.5%)		9 (50.0%)	
Purely liquid	2 (4.9%)	1 (1.9%)		1 (5.6%)	
<b>Mass:Psoas Ratio-median (IQR)</b>	0.7 (0.6-0.9)	1.1 (1.0-1.2)	<b>&lt;0.0001</b>	1.05 (1-1.2)	<b>&lt;0.0001</b>
<b>Lesion comparison for patients with a uterus</b>	<b>(n= 36)</b>	<b>(n=43)</b>		<b>(n=17)</b>	
<b>Mass:Uterus Ratio - median (IQR)</b>	0.5 (0.5-0.7)	0.9 (0.7-1.0)	<b>&lt;0.001</b>	0.8 (0.7-1)	<b>0.0001</b>
<b>Enhancement compared to uterus –n(%)</b>			<b>&lt;0.001</b>		<b>0.002</b>
Hyperdense	0 (0%)	2 (4.7%)		0	
Isodense	6 (16.7%)	29 (67.4%)		11 (61.1%)	
Hypodense	30 (83.3%)	12 (27.9%)		7 (38.9%)	

**Table 2:** Comparison of CT characteristics in Fibrothecoma and SPC tumours. *n* = number of lesions

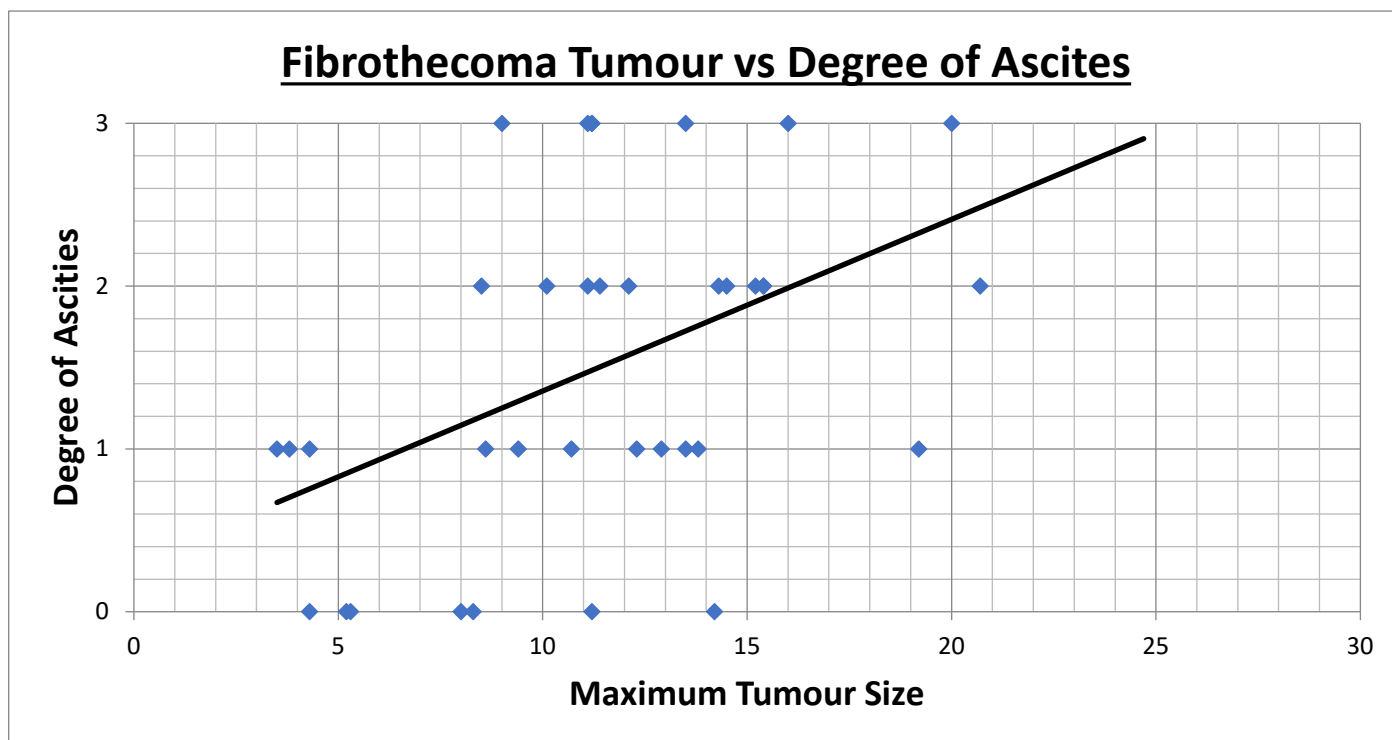


**Figure 9:**

Scatter graph demonstrating a positive correlation between fibrothecoma tumour sizes and the degree of ascites. **0** – No ascites, **1** – Mild ascites (fluid in the subhepatic spaces), **2** – Moderate ascites (fluid in the subphrenic space, perisplenic and pelvis), **3** – Significant ascites (distended abdomen with intra-abdominal fluid surrounding the mesentery)

Spearman's correlation coefficient ( $r$ ) = 0.49,  $p=0.0012$

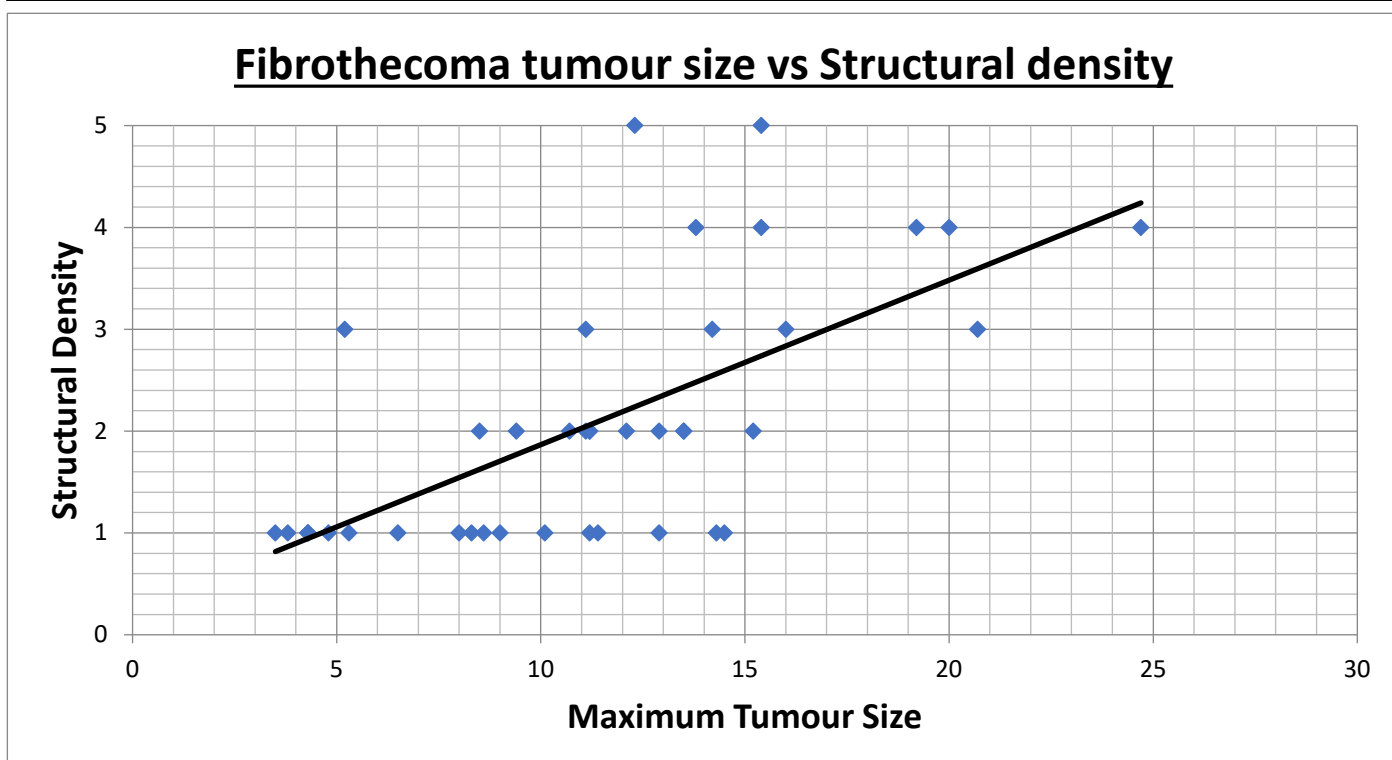


**Figure 5:**

Scatter graph demonstrating positive correlation between the size of the fibrothecoma tumour and its tendency to adopt a more cystic structural configuration.

Spearman's correlation coefficient ( $r$ ) = 0.66,  $p<0.001$

<b>Table 4</b>	
<b>CT Findings</b>	<b>Ovarian Endometrioids Lesions (n = 15)</b>
<b>Size - median (IQR)</b>	11 (8.9-14.6)
<b>Shape- n(%)</b>	
Lobulated	10 (66.7%)
Oval	4 (26.7%)
Round	1 (6.6%)
<b>Margins – n(%)</b>	
Well-defined	15 (100%)
Ill-defined	0 (0%)
<b>Calcification in lesion – n(%)</b>	
Yes	1 (6.7%)
No	14 (93.3%)
<b>Density – n(%)</b>	
Purely Solid	0
Predominantly Solid	3 (20.0%)
Mixed	4 (26.7%)
Predominantly Cystic	8 (53.3%)
Purely liquid	0
<b>Mass:Psoas Ratio-median (IQR)</b>	1.1 (1.0-1.3)
<b>Mass:Uterus Ratio - median (IQR)</b>	0.8 (0.7-0.9)
<b>Enhancement to uterus –n(%)</b>	
Hyperdense	0 (0%)
Isodense	7 (46.7%)
Hypodense	8 (53.3%)

**Table 4 – CT Features demonstrated in ovarian endometrioids**

## Discussion

Ovarian fibrothecoma are benign neoplasms that are commonly mistaken radiologically as malignant tumours<sup>(7,8,28)</sup>. To our knowledge, this study contains the largest number of pathologically proven fibrothecomas with the interest of CT image analysis. Serous ovarian tumours such as SPCs belong to a subgroup of serous epithelial cell neoplasms. They both share common signs and symptoms including high oestrogen levels, menstrual disorder, abdominal distention and vaginal bleeding<sup>(5,6)</sup>.

Typical modalities used for assessing diseases of this group include ultrasound, CT and MRI. Ultrasound is convenient and is effective in determining the presence of large ovarian lesions<sup>(29,30)</sup>. However they lack definitive resolution, qualitative diagnosis and the acquired images are usually limited by the skill of the operator<sup>(31)</sup>. On MRI, these typically exhibit hypo- to isointensity on T1 and T2 weighted images on comparison with the myometrium<sup>(32,33)</sup>. MRI provides excellent qualitative diagnosis as some adjacent tumours may demonstrate cystic and haemorrhagic degeneration. MRI is an invaluable tool for troubleshooting however these investigations often come with significant drawbacks such as lengthy acquisition times, claustrophobia and MRI unsafe metallic implants. In recent decades, CT has become exponentially efficient demonstrating high level imaging quality without heavy radiation trade-offs<sup>(34)</sup>. Although CT alone will not replace the role MRI troubleshooting, CT characteristics of fibrothecoma are still worthy of note as CT studies are usually the initial encounter of ovarian masses. Benign entities should be considered prior to premature referrals to tertiary onco-gynaecological centres.

Attention to other common adnexal masses should not be overlooked when forming differential diagnoses for fibrothecomas. Mucinous ovarian masses usually differ greatly in their multilocular septated, heavily cystic appearance. Metastatic ovarian involvements are vastly bilateral. They tend to present with lymphovascular invasion and are typically small in comparison to primary ovarian neoplasm<sup>(28,35)</sup>. Benner tumours, similar with fibromas, commonly adopt fibrous rubbery consistency with well circumscribed, solid appearance. However fibrothecoma are typically large as Brenner tumours tend to be <2cm<sup>(3,28,36)</sup>. Pedunculated leiomyomas can present with haemorrhagic or cystic degeneration appearances. These may occur in close proximity with the ovary resulting in diagnostic ambiguity. Clues such as vessel bridging, parenchymal stalk and heterogeneous enhancement can provide added value even on CT (**Figure 7**). Another potential differential include cystadenofibromas which too include both cystic and solid components. However in cystadenofibromas, the cystic component are typically strongly predominated in comparison to the solid component<sup>(37)</sup>. Fibrothecomas tend to favour solid component predominance as opposed to cystic<sup>(38)</sup>.

Both patient cohorts mostly fell within the fifth and sixth decade, matching the data reported in literature<sup>(1,28,31,39)</sup>. As expected from the fibrothecoma arm, our study confirms that lymphadenopathy and peritoneal disease are rarely associated with this type of benign tumour<sup>(40,41)</sup>. The peritoneal disease recorded within the fibrothecoma arm represented mild, non-specific fat stranding (**Figure 8**). In contrast, a third of the SPC cohort had positive signs of lymphadenopathy and peritoneal disease (33.3% and 72.2% respectively) ( $p < 0.001$ ).

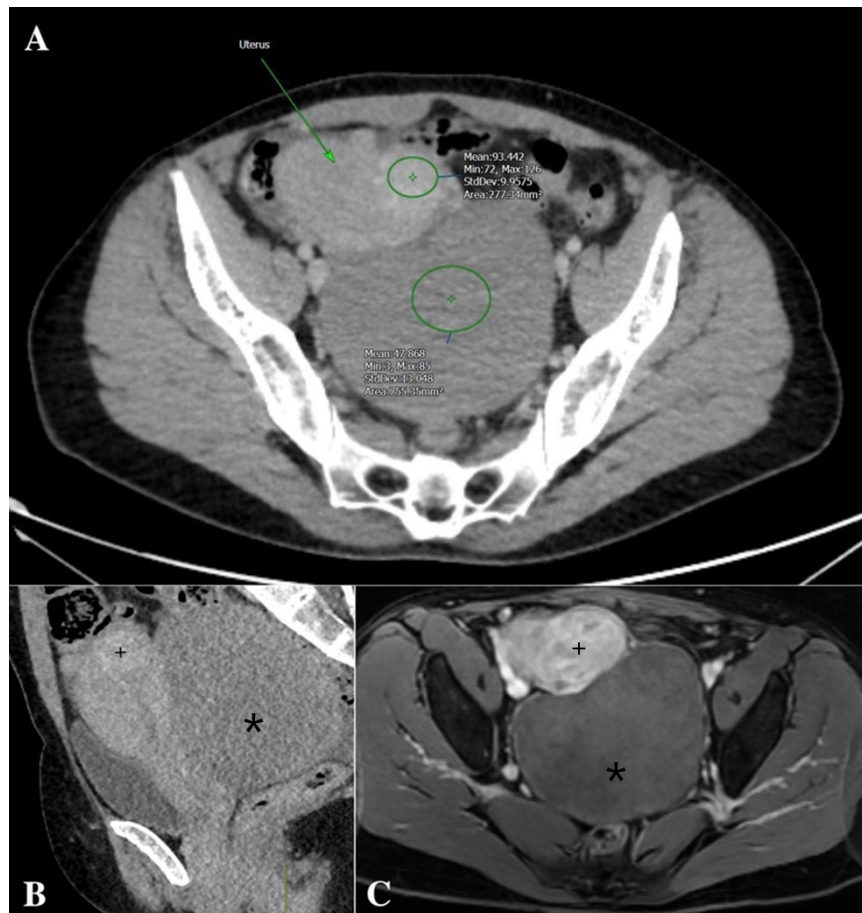


**Figure 7: Matching CT and MRI Comparison of fibrothecoma and a large leiomyoma**

A – CT axial study demonstrating prominent enhancement of the uterus in comparison to the leiomyoma (Denoted by the Top ROI. Bottom ROI denotes HU of fibrothecoma mass).

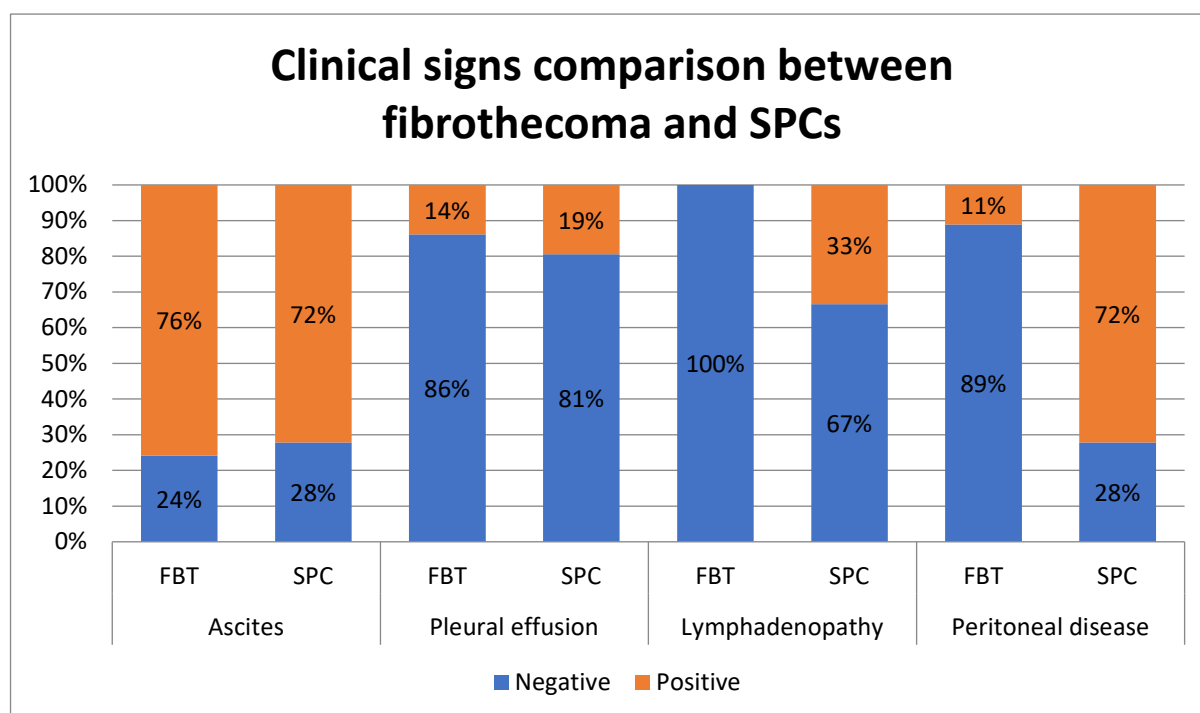
B – CT sagittal slice of the large fibrothecoma (Denoted by the asterisk, \*) and the uterus (Denoted by the plus symbol, +)

C – MRI T1 post contrast axial slice of the heterogenous, hyperintense uterus in comparison to the large fibrothecoma mass

Other clinical manifestations such as pleural effusion and ascites were seen in both cohorts. These signs in benign ovarian tumours are well-documented in literature with the known phenomenon of Meigs syndrome<sup>(7,28)</sup>. Our findings agree with the literature that the larger the ovarian tumour, the more likely symptoms become more apparent (**Figure 9**)<sup>(2,6,10,31,32)</sup>. CA-125 tumour markers are commonly used as a representation of malignancy. In this study, 58.3% of fibrothecoma had raised CA-125 levels which is suggestive that tumour markers do not always provide an accurate representation of malignancy<sup>(10,31)</sup>.

It should also be noted that despite some cases being labelled histologically FIGO stage 3, significant delay between date of diagnosis on CT and date of the surgery was sometimes observed, with one patient experiencing a delay of 9 months from diagnosis to surgery (Median:97 days, Range:[8-275 days]).



**Figure 8:**

Split proportion of fibrothecoma (FBT) and SPC patients in relation to their corresponding clinical signs.

Presence of ascites is common in both cohorts however there is a higher probability that other clinical signs would be present in patients with SPC

Our study has shown a positive correlation between larger tumours and central necrotic appearances ( $p=0.001$ ) which is in agreement with both Chen and Zhang's observation<sup>(2,32)</sup>. Although mixed solid and cystic components of fibrothecoma lesions were sometimes observed, our study demonstrates that purely solid ovarian tumours are more likely to indicate a fibrothecoma rather than SPC. Conversely, predominantly cystic tumours are strongly correlated with SPCs, with a decreasing trend of occurrence as the tumour becomes more solid (**Figure 6**) ( $p<0.001$ ). Many reports in literature agree on the solid configuration of fibrothecoma tumours<sup>(1,29,31,39)</sup>. Ovarian high-grade serous carcinoma (HGSC), Ma et al. showed 87% of their primary HGSC tumours had demonstrated mixed multilocular cystic-solid to solid components. This suggests HGSCs tend to adopt mixed-solid tumour configurations rather than purely cystic features<sup>(42)</sup>.

On the matter of presence of calcification, these did not exhibit statistically significant differences ( $p>0.05$ ) between ovarian fibrothecomas and SPCs. In terms of shape, it appears fibrothecoma tend to adopt a variety of shapes whereas SPCs are typically lobulated ( $p=0.001$ ), in keeping with the literature<sup>(6,23,28,43)</sup>.

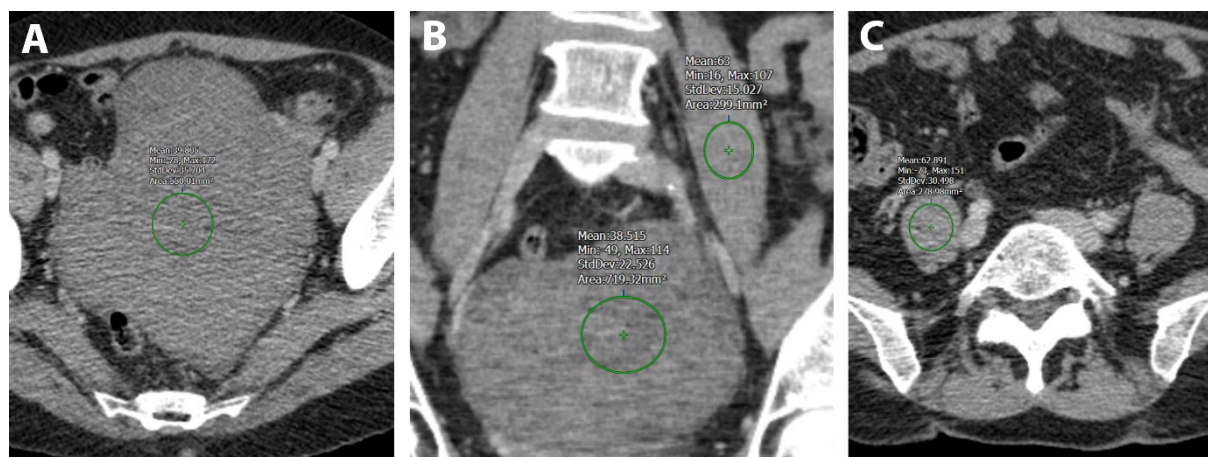


**Figure 10:** Fibrothecoma (solid component) vs Psoas HU ratio comparison.

A – Axial section of fibrothecoma mass. B – Coronal section of fibrothecoma mass and psoas muscle. C – Axial section of the psoas muscle

*Mean HU of psoas – 63. Mean HU of fibrothecoma mass – 38*

In cases of fibrothcoma, the ratio value is likely to be less than 1.

Interrogating tumours via CT HU has been widely reported in literature for a multitude of body systems<sup>(44–46)</sup>. We introduced a simple novel approach of analysis by selecting a minimally-varying internal reference, such as the psoas muscle or the uterus, to calculate an arbitrary ratio value. By measuring the HU value alone, we demonstrated the range of the fibrothecoma mass to lie within the range of 24 to 66 (Mean average  $44 \pm 11.2$ ). Comparison of *mass:psoas* or *mass:uterus* ratio values show a statistically significant difference between the 2 cohorts. If the arbitrary ratio value is  $<1$ , the tumour is likely to represent fibrothecoma ( $p < 0.001$ ) (**Figure 10**). Conversely, if the ratio value of  $>1$ , there's significant probability of the tumour being an SPC ( $p < 0.001$ ) (**Figure 11**). This is true regardless of whether the psoas or uterus is used as a reference.

It is unsurprising that the SPC arm included radiological features of widespread metastasis and thus the question of benignity poses no confusion. However, as previously mentioned, there were cases of 'SPCs mimicking fibrothecoma' demonstrating indeterminate appearances and thus its aggressive nature. This small cohort comprising of 12 patients (18 lesions) also showed many similarities when compared to the main cohort including cystic component predominance, *mass:psoas/mass:uterus* ratio disassociation and presence of Meig's syndrome (**Table 1** and 3).

In regards to laterality, fibrothecomas has a tendency for unilateral presentations similar to the results demonstrated by Zhang et al<sup>(2,32)</sup>. Bilateral presentations is shown to be favoured by SPCs, agreeing with the literature<sup>(28)</sup>.

Our secondary aim was to include radiological comparisons of ovarian endometrioids however it was decided that a total of 13 patients (15 lesions) was an insufficient sample size to provide statistically-reliable analyses (**Table 4**). Interestingly, the internal reference ratio comparison also showed a median value of 1.1 (IQR 1.02–1.4), a value  $>1$  providing a possible indicator for malignancy.

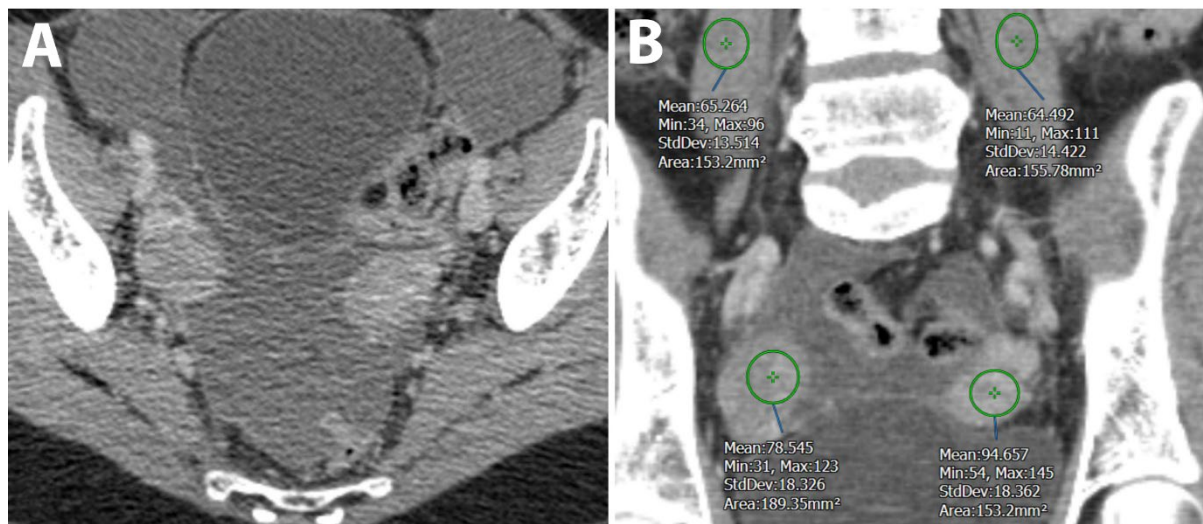


**Figure 11:** SPC (solid component) vs Psoas HU ratio comparison.

A – Axial image demonstrating bilateral ovarian SPC tumour. B – Image 9B denoting the HU value of the tumour and psoas muscle in coronal view.

In cases of SPCs, when *equation 1* is applied, the ratio value is likely to be **greater than 1**.

Our study showed limitations across the following areas: ①Assessment for each individual lesion was only viewed by one uro-gynaecological consultant radiologist and one radiology registrar, thereby increasing the risk of view-bias. ②Our novel approach required the usage of various structures (psoas and uterus) as an internal reference, which can show a degree of anatomical variation and may unintentionally affect interpretation. ③This was a retrospective, observational study. However, as fibrothecomas are typically rare, it would be impractical to perform a prospective study given the limited timeframe. ④There are matching cohort numbers of fibrothecoma and SPCs patients and although there should be significantly higher samples of SPCs, the fibrothecoma data was gathered across three sites over the one Trust. The SPC samples were only obtained in one site and despite this; there remains more lesions of SPCs in comparison to fibrothecoma. ⑤Many patients within the SPC cohort demonstrated disseminated disease, clearly showing the malignant nature of the tumours rather than being a mimic of benign fibrothecomas. However, of those that did not show obvious disseminated disease, the data continued to show statistically significant results when compared with fibrothecoma.

## Conclusion

A diagnosis of fibrothecoma should be considered on CT-imaging if the following features are observed: solid tumour configurations, unilaterality, lack of lymphadenopathy or peritoneal involvement and mass to internal reference density ratio of <1. We believe this novel approach does not exclude the necessity of MRI evaluation of ovarian tumours however it is a useful adjunct for early detection of fibrothecoma tumours thereby reducing unnecessary tertiary gynae-oncological unit referrals. This ultimately reduces the workload for MDMs, financial burdens and patient physical morbidity from undue stress and anxiety related to erroneous cancer diagnosis or unnecessary complex surgery.

## Reference:

1. Troiano RN, Lazzarini KM, Scoutt LM, Lange RC, Flynn SD, McCarthy S. Fibroma and fibrothecoma of the ovary: MR imaging findings. *Radiology*. 1997 Sep;204(3):795–8.
2. Zhang Z, Wu Y, Gao J. CT Diagnosis in the Thecoma–Fibroma Group of the Ovarian Stromal Tumors. *Cell Biochem Biophys*. 2014;71(2):937–43.
3. Shinagare AB, Meylaerts LJ, Laury AR, Morteale KJ. MRI features of ovarian fibroma and fibrothecoma with histopathologic correlation. *Am J Roentgenol*. 2012 Mar;198(3).
4. Chen VW, Ruiz B, Killeen JL, Coté TR, Wu XC, Correa CN. Pathology and classification of ovarian tumors. *Cancer*. 2003 May;97(10 Suppl):2631–42.
5. Kurman RJ, Carcangiu ML, Herrington CS YR. Classification of tumours of the ovary. 4th ed. Vol. 6, WHO Classification of Tumours. 2014. 44–56 p.
6. Horta M, Cunha TM. Sex cord-stromal tumors of the ovary: A comprehensive review and update for radiologists. Vol. 21, Diagnostic and Interventional Radiology. AVES Ibrahim Kara; 2015. p. 277–86.
7. Chung KC, Lee HH, Su MH, Chang WH, Lai WA, Wang PH. Ovarian fibrothecoma mimicking ovarian cancer: Using laparoscopy to avoid unnecessary exploratory laparotomy. Vol. 58, Taiwanese Journal of Obstetrics and Gynecology. Elsevier Ltd; 2019. p. 903–4.
8. Cho YJ, Lee HS, Kim JM, Joo KY, Kim M La. Clinical characteristics and surgical management options for ovarian Fibroma/Fibrothecoma: A Study of 97 Cases. *Gynecol Obstet Invest*. 2013;76(3):182–7.
9. Shanbhogue AKP, Shanbhogue DKP, Prasad SR, Surabhi VR, Fasih N, Menias CO. Clinical syndromes associated with ovarian neoplasms: a comprehensive review. *Radiogr a Rev Publ Radiol Soc North Am Inc*. 2010;30(4):903–19.
10. Bazot M, Ghossain MA, Buy JN, Deligne L, Hugol D, Truc JB, et al. Fibrothecomas of the ovary: CT and US findings. *J Comput Assist Tomogr*. 1993;17(5):754–9.
11. Tamai K, Koyama T, Saga T, Kido A, Kataoka M, Umeoka S, et al. MR features of physiologic and benign conditions of the ovary. *Eur Radiol [Internet]*. 2006;16(12):2700–11. Available from: <https://doi.org/10.1007/s00330-006-0302-6>
12. Oh SN, Rha SE, Byun JY, Lee YJ, Jung SE, Jung CK, et al. MRI features of ovarian fibromas: emphasis on their relationship to the ovary. *Clin Radiol*. 2008 May;63(5):529–35.
13. Limb M. Sharp rise in CT scans prompts call for new safeguards on radiation exposure. *BMJ [Internet]*. 2014;349. Available from: <https://www.bmj.com/content/349/bmj.g5218>
14. Kim HJ, Kim JK, Cho K-S. CT Features of Serous Surface Papillary Carcinoma of the Ovary. *Am J Roentgenol [Internet]*. 2004 Dec 1;183(6):1721–4. Available from: <https://doi.org/10.2214/ajr.183.6.01831721>
15. Kim SH, Cho JY, Park IA, Kang SB, Lee HP, Han MC. Radiological findings in serous surface papillary carcinoma of the ovary: Case reports. *Acta radiol [Internet]*. 1997 Sep 1;38(5):847–9. Available from: <https://doi.org/10.1080/02841859709172422>
16. Chopra S, Laurie LR, Chintapalli KN, Valente PT, Dodd GDIII. Primary Papillary Serous Carcinoma of the Peritoneum: CT-Pathologic Correlation. *J Comput Assist Tomogr [Internet]*. 2000;24(3). Available from:

- [https://journals.lww.com/jcat/Fulltext/2000/05000/Primary\\_Papillary\\_Serous\\_Carcinoma\\_of\\_the.7.aspx](https://journals.lww.com/jcat/Fulltext/2000/05000/Primary_Papillary_Serous_Carcinoma_of_the.7.aspx)
17. Furukawa T, Ueda J, Takahashi S, Higashino K, Shimura K, Tsujimura T, et al. Peritoneal serous papillary carcinoma: radiological appearance. *Abdom Imaging* [Internet]. 1999;24(1):78–81. Available from: <https://doi.org/10.1007/s002619900446>
  18. Jemal A, Siegel R, Xu J, Ward E. Cancer statistics, 2010. *CA Cancer J Clin*. 2010;60(5):277–300.
  19. Jelovac D, Armstrong DK. Recent progress in the diagnosis and treatment of ovarian cancer. *CA Cancer J Clin* [Internet]. 2011/04/26. 2011;61(3):183–203. Available from: <https://pubmed.ncbi.nlm.nih.gov/21521830>
  20. Terada T. Endometrioid adenocarcinoma of the ovary arising in atypical endometriosis. *Int J Clin Exp Pathol* [Internet]. 2012/10/20. 2012;5(9):924–7. Available from: <https://pubmed.ncbi.nlm.nih.gov/23119109>
  21. Valenzuela P, Ramos P, Redondo S, Cabrera Y, Alvarez I, Ruiz A. Endometrioid adenocarcinoma of the ovary and endometriosis. *Eur J Obstet Gynecol Reprod Biol*. 2007 Sep;134(1):83–6.
  22. Foreman J. From the Archives of the Archives. *Arch Ophthalmol*. 1992;110(12):1713.
  23. Wagner BJ, Buck JL, Seidman JD, McCabe KM. From the archives of the AFIP. Ovarian epithelial neoplasms: radiologic-pathologic correlation. *Radiogr a Rev Publ Radiol Soc North Am Inc*. 1994 Nov;14(6):1351–6.
  24. Tanaka YO, Yoshizako T, Nishida M, Yamaguchi M, Sugimura K, Itai Y. Ovarian Carcinoma in Patients with Endometriosis. *Am J Roentgenol* [Internet]. 2000 Nov 1;175(5):1423–30. Available from: <https://doi.org/10.2214/ajr.175.5.1751423>
  25. Mazzaferro V, Majno P. Principles for the best multidisciplinary meetings. *Lancet Oncol*. 2011 Apr;12(4):323–5.
  26. Leng G. The National Institute for Health and Clinical Excellence: an interview with Gillian Leng, MD. *Qual Manag Health Care*. 2007;16(3):293–6.
  27. De Ieso PB, Coward JI, Letsa I, Schick U, Nandhabalan M, Frentzas S, et al. A study of the decision outcomes and financial costs of multidisciplinary team meetings (MDMs) in oncology. *Br J Cancer*. 2013 Oct 29;109(9):2295–300.
  28. Taylor EC, Irshaid L, Mathur M. Multimodality Imaging Approach to Ovarian Neoplasms with Pathologic Correlation. *RadioGraphics* [Internet]. 2020;2019(2):200086. Available from: <http://pubs.rsna.org/doi/10.1148/rg.2021200086>
  29. Paladini D, Testa A, Van Holsbeke C, Mancari R, Timmerman D, Valentin L. Imaging in gynecological disease (5): Clinical and ultrasound characteristics in fibroma and fibrothecoma of the ovary. *Ultrasound Obstet Gynecol*. 2009;34(2):188–95.
  30. Scully RE. *Histological Typing of Ovarian Tumours* [Internet]. Springer Berlin Heidelberg; 1999. Available from: <https://doi.org/10.1007/978-3-642-58564-7>
  31. Yen P, Khong K, Lamba R, Corwin MT, Gerscovich EO. Ovarian Fibromas and Fibrothecomas. *J Ultrasound Med*. 2013;32(1):13–8.
  32. Chen J, Wang J, Chen X, Wang Y, Wang Z, Li D. Computed tomography and magnetic resonance imaging features of ovarian fibrothecoma. *Oncol Lett*. 2017;14(1):1172–8.
  33. Chung BM, Park S Bin, Lee JB, Park HJ, Kim YS, Oh YJ. Magnetic resonance imaging features of

- ovarian fibroma, fibrothecoma, and thecoma. *Abdom Imaging*. 2015 Jun 1;40(5):1263–72.
34. Willemink MJ, Noël PB. The evolution of image reconstruction for CT—from filtered back projection to artificial intelligence. *Eur Radiol*. 2019;29(5):2185–95.
  35. Marko J, Marko KI, Pachigolla SL, Crothers BA, Mattu R, Wolfman DJ. Mucinous neoplasms of the ovary: Radiologic-pathologic correlation. *Radiographics*. 2019;39(4):982–97.
  36. Costerira F, Felix A, Cunha Margarida. Brenner tumours. *The British Journal of Radiology*. 2022. 59:1130.  
Available from: <https://www.birpublications.org/doi/abs/10.1259/bjr.20210687>
  37. Virgilio BA, De Blasis I, Sladkevicius P, Moro F, Zannoni GF, Arciuolo D, et al. Imaging in gynecological disease (16): clinical and ultrasound characteristics of serous cystadenofibromas in adnexa. *Ultrasound Obstet Gynecol*. 2019;54(6):823–30.
  38. Wu B, Peng WJ, Gu YJ, Cheng YF, Mao J. MRI diagnosis of ovarian fibrothecomas: Tumour appearances and oestrogenic effect features. *Br J Radiol*. 2014 Jun 1;87(1038).
  39. Sivanesaratnam V, Dutta R, Jayalakshmi P. Ovarian fibroma — clinical and histopathological characteristics. *Int J Gynecol Obstet* [Internet]. 1990 Nov 1;33(3):243–7. Available from: [https://doi.org/10.1016/0020-7292\(90\)90009-A](https://doi.org/10.1016/0020-7292(90)90009-A)
  40. Gaddey HL, Riegel AM, Bergquist E, Medicine F, Program R, Air O, et al. Evaluation of Unexplained Lymphadenopathy. *Am Fam Physician*. 2016;94(11):896–903.
  41. Kyriazi S, Kaye SB, deSouza NM. Imaging ovarian cancer and peritoneal metastases—current and emerging techniques. *Nat Rev Clin Oncol* [Internet]. 2010;7(7):381–93. Available from: <https://doi.org/10.1038/nrclinonc.2010.47>
  42. Ma FH, Qiang JW, Zhang GF, Li HM, Cai SQ, Rao YM. Magnetic resonance imaging for distinguishing ovarian clear cell carcinoma from high-grade serous carcinoma. *J Ovarian Res* [Internet]. 2016;9(1):1–8. Available from: <http://dx.doi.org/10.1186/s13048-016-0251-x>
  43. Outwater EK, Wagner BJ, Mannion C, McLarney JK, Kim B. Sex cord-stromal and steroid cell tumors of the ovary. *RadioGraphics*. 1998;18(6):1523–46.
  44. Choi Y, Gil BM, Chung MH, Yoo WJ, Jung NY, Kim YH, et al. Comparing attenuations of malignant and benign solitary pulmonary nodule using semi-automated region of interest selection on contrast-enhanced CT. *J Thorac Dis*. 2019;11(6):2392–401.
  45. McGahan JP, Sidhar K, Fananapazir G, Early H, Corwin MT, Silverman SG, et al. Renal cell carcinoma attenuation values on unenhanced CT: importance of multiple, small region-of-interest measurements. *Abdom Radiol (New York)*. 2017 Sep;42(9):2325–33.
  46. Urata M, Kijima Y, Hirata M, Shinden Y, Arima H, Nakajo A, et al. Computed tomography Hounsfield units can predict breast cancer metastasis to axillary lymph nodes. *BMC Cancer* [Internet]. 2014;14(1):730. Available from: <https://doi.org/10.1186/1471-2407-14-730>